Machine Learning based Approach to include Production Related Variations in the Simulation of Magnetic Sensors

Hagen Schmidt, Tim Becker, Jörg Seewig

Institute for measurement and sensor technology
RPTU Kaiserslautern-Landau
Gottlieb-Daimler-Straße 47
67663 Kaiserslautern
h.schmidt@mv-rptu.de
t.becker@rptu.de
j.seewig@mv.rptu.de

Abstract: Simulations are an important tool in the development and design of magnetic sensors. The disadvantage of these simulations lies in frequent assumption of perfect conditions, without considering production-related variations. Depending on the system, these variations can have a significant effect on the sensor output signals, leading to an offset between simulation and reality. Running multiple simulations to cover all variations is often too time consuming. This weakness is addressed in this study.

Machine learning techniques are used to train a model on production-related variations with simulated data. The model is then able to predict sensor signal deviations in real time based on the ideal signals. This allows designers to check their sensor design within the specified production variations without the need for additional time-consuming simulations.

The approach is implemented using a virtual module of a supporting magnet and a GMR sensor array called GLM712 from Sensitec GmbH. This type of sensor is used to detect the angle of rotation and speed of tooth structures without contact. A characteristic of this type of sensor technology is the need for a specific design depending on the geometry of the tooth structure. In the manufacturing of these sensors, there are variations in sensor position, orientation and the properties of the supporting magnet, which have been shown to affect the signal. These are the variations for which the machine learning model is trained.

1. Introduction

In the design and investigation of sensor systems, simulations are an essential tool for generating emulated signals. Often, the required amount of data cannot be produced with the necessary level of variation using real-world measurements at a reasonable cost. Key system parameters, such as geometry, are fixed in real systems and can either not be varied at all or only with significant material and time expenditures.
A critical limitation of simulations is the assumption of ideal manufacturing conditions, ignoring production-induced variations such as deviations in sensor positioning, orientation, and properties. In reality, manufacturing tolerances can cause significant discrepancies between simulated and actual sensor outputs, affecting system performance and reliability.
One approach to address this limitation is to perform multiple simulations that account for all possible variations, but this can also be extremely time-consuming and computationally intensive. This challenge highlights the need for efficient methods to predict and compensate for production-related variations in sensor outputs without relying on extensive simulation efforts.

This paper introduces a machine learning (ML) based approach to predict sensor signal deviations caused by manufacturing tolerances efficiently. By training a model on data derived from ideal simulations augmented with systematic variations representing production tolerances, the approach enables real-time prediction of sensor performance under various manufacturing conditions. This methodology significantly reduces the reliance on extensive simulations and accelerates the sensor design and validation process.

The proposed approach is validated using a simulated system of a soft magnetic gear, a magnet and a giant magnetoresistance (GMR) sensor array. In this specific use case, the gear rotates and modulates the magnetic field provided by the magnet. The GMR sensor array, designated as GLM712 from the manufacturer Sensitec GmbH, is placed between the magnet and the gear and detects the changes in magnetic field strength caused by the rotating gear. The sensor contains 16 GMR elements, which are configured into two measurement bridges (where 2 GMR elements are connected together in series). The measurement bridge voltage is tapped at the sensor output, and two phase-shifted sinusoidal signals indicate the rotational movement of the gear. Manufacturing-related deviations in the placement of the GMR elements and the properties of the magnet affect these signals.

The study considers various gear geometries and systematically incorporates manufacturing tolerances of the sensor-magnet-subsystem into the simulation data. An Extreme Gradient Boosting (XGBoost) model is trained and optimized to predict the impact of these variations to the sensor signals accurately. The results demonstrate the model's effectiveness in maintaining high prediction accuracy while offering substantial reductions in simulation time and computational resources.

2. Related Work and Applications

The integration of ML techniques with traditional simulation methods has emerged as a powerful strategy in enhancing predictive modeling across various engineering domains. This hybrid approach addresses limitations associated with both data limitations and high computational costs, offering improved accuracy and efficiency in complex system analyses.
Several studies have demonstrated the effectiveness of combining simulation with ML for fault detection and system diagnostics. For instance, Gao et al. (2021) proposed a hybrid method that integrates Finite Element Method (FEM) simulations with Generative Adversarial Networks (GANs) to generate additional fault samples, thereby improving classification accuracy in rotor-bearing systems [GLHX21]. This approach effectively leverages simulated data to compensate for the lack of real-world fault data, enhancing the robustness of the diagnostic model.
Liu et al. (2020) introduced a personalized diagnosis method employing FEM simulations to create training datasets for Support Vector Machine (SVM) models, enabling accurate fault detection in mechanical components despite limited available fault data [LiHX20]. This method underscores the critical role of simulation in supplementing ML models when empirical data is insufficient or challenging to obtain. In addressing computational efficiency, Ahamed and Uddin (2023) presented a two-step ML framework that reduces the dependence on extensive simulations for exploring complex physical systems. By initially training on a limited set of high-fidelity simulations and subsequently refining predictions through ML models, this approach achieves substantial reductions in computational time without compromising accuracy [AhUd23]. Furthermore, Wang et al. (2022) investigated the application of ML models trained on simulation data for fault detection in gear mechanisms. Utilizing a lumped parameter model to generate training samples, the study achieved near-perfect accuracy in fault classification, demonstrating the practicality and effectiveness of integrating simulation data with advanced learning algorithms in real-world applications [WaYX22].

Despite these advancements, limited research has focused specifically on predicting production-induced variations in sensor outputs using ML. Existing studies primarily address fault detection and general system diagnostics but do not extensively explore manufacturing tolerances' impact on sensor performance. This research aims to fill this gap by developing a ML model tailored to predict sensor signal deviations resulting from production-related variations, thereby enhancing the accuracy and efficiency of sensor design and validation processes.

3. Methods

This chapter outlines the approaches and tools employed to simulate, analyze, and model the behavior of a GMR sensor under varying manufacturing tolerances, providing a comprehensive framework for data generation, feature extraction, and ML model development.

3.1 Simulation Software

GMR sensor design relies on simulation techniques, particularly the Finite Element Method (FEM), to calculate an approximation of a magnetic field and to predict sensor behaviour under different operational scenarios [ReCR09]. The simulations in this study are carried out by a software developed at the

University of Kaiserslautern-Landau (RPTU) in cooperation with Sensitec GmbH[1]. The software is capable of calculating the magnetic field for different geometric problem settings with various hard-magnetic objects. Additionally, virtual versions of the GMR sensor array and the Hall sensor are included, which compute the sensor output signals based on the approximated magnetic field.

In this software, the geometric description of the three-dimensional system geometry is carried out using the methods of Constructive Solid Geometry (CSG). A major advantage of CSG is its automatability through algorithms. A function created once for generating a specific geometry can produce any number of similar geometries by adjusting its parameters. For example, arbitrary gear geometries can be generated by specifying just a few parameters, such as diameter, length, number of teeth, tooth height, and tooth width.
To calculate the magnetic field, the weak form

$$\int_{\Omega} (\vec{\nabla} \times \vec{A}) \cdot (\vec{\nabla} \times \vec{v}) d\Omega = \mu \int_{\Omega} \vec{M} \cdot (\vec{\nabla} \times \vec{v}) d\Omega$$

of the magnetostatic boundary value problem

$$\Delta \vec{A} = -\mu \vec{\nabla} \times \vec{M}$$

is formulated and solved for the described geometry, where $\vec{A}$ is the vector potential, $\vec{M}$ is the magnetization, μ is the magnetic permeability, and $\vec{v}$ is the test function within the bounded domain Ω.
The boundary conditions are set as Neumann boundary conditions

$$\frac{\partial \vec{A}}{\partial \vec{n}} = 0$$

where $\vec{n}$ is the normal vector.

For performing the calculations, a powerful software package is used. NGSolve, developed at the TU Wien (Vienna) and other universities, provides extensive functionalities for finite element method (FEM) computations in mechanics, fluid dynamics, and electromagnetics [Schö14].

An integral part of the package is a 2D/3D mesh generator called NETGEN [Schö97]. It automatically generates the required mesh for FEM calculations based on the described CSG geometry. The mesh consists exclusively of first-order tetrahedral elements with a maximum edge length of h.

The generated mesh enables the L2-projection of the continuous problem into a discrete system. The resulting linear system of equations is preconditioned and solved iteratively using the gradient descent method, until a configurable error tolerance threshold is met, yielding the approximation of the vector potential $\vec{A}^h$.

The final result is the numerically computed magnetic flux density and field strength

$$\vec{B}^h = \vec{\nabla} \times \vec{A}^h \text{ und } \vec{H}^h = \frac{1}{\mu} \vec{\nabla} \times \vec{B}^h - \vec{M}^h.$$

The calculated magnetic field serves as the basis for designing the virtual GMR sensor array. Fig. 1 and Fig. 2 illustrate a simplified structure and a simplified circuit diagram of the sensor, where two of the 16 elements connected in series have already been combined into one element.

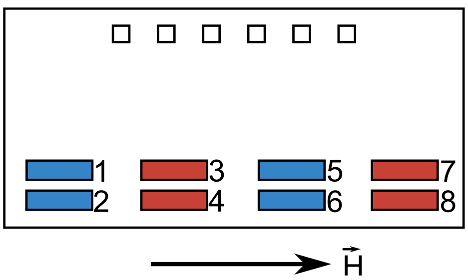

Fig. 1: Simplified arrangement of the GMR elements

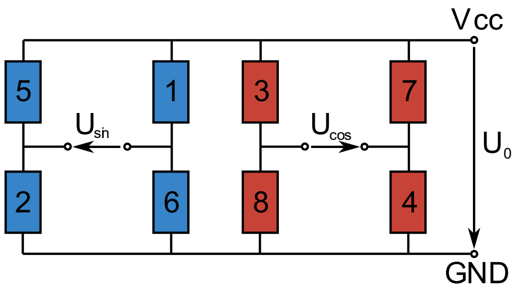

Fig. 2: Circuit diagram of the GMR elements

[1] https://doi.org/10.5281/zenodo.8414074

The sensor output signals are labeled as U_{sin} and U_{cos}. These names arise from the $90°$ phase shift between the two signals, resulting from the arrangement.
GMR elements change their electrical resistance depending on the applied magnetic field in the direction of $\vec{H}$ in Fig. 1. The relationship between resistance and magnetic field strength is described by a characteristic curve

$$R_i = -1{,}26 \cdot 10^{-6}\Omega \cdot \vec{H}_i^h \cdot \frac{m}{A} + 1{,}442\Omega$$

where R_i is the resistance of the GMR element $i \in 1 \ldots 8$ and $\vec{H}_i^h$ is the approximated magnetic field strength affecting the element. In this study, the characteristic curve is provided in a linearized form only. The actual characteristic curve is a trade secret of Sensitec GmbH and was available for this study.

According to the bridge circuits shown in Fig. 2, the sensor output signals are calculated as

$$U_{sin} = \left(\frac{R_5 + R_6}{R_1 + R_2 + R_5 + R_6} - \frac{R_1 + R_2}{R_1 + R_2 + R_5 + R_6}\right) \cdot U_0$$
$$U_{cos} = \left(\frac{R_3 + R_4}{R_3 + R_4 + R_7 + R_8} - \frac{R_7 + R_8}{R_3 + R_4 + R_7 + R_8}\right) \cdot U_0$$

where U_0 is the supply voltage.

3.2 Collection of Measurement Data including Manufacturing Tolerances

Using the simulation software in the previous section, simulations were carried out to record the signal deviations in the case of deviations in the sensor/magnet system. Fig. 3 illustrates a simplified section of the simulation space. The relevant gear dimensions, such as tooth height, tooth width, and the circle diameter, are also depicted in the figure, which provides a basis for understanding the parameterized geometry.

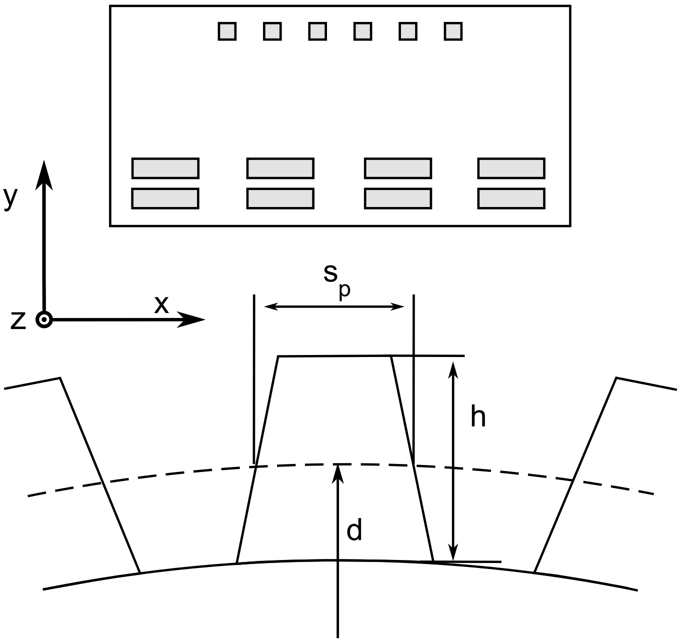

Fig. 3: Simplified section of the simulation domain illustrating the spatial arrangement of the sensor and gear relative to the coordinate system.

To generate a diverse dataset, 250 unique gear geometries were created by systematically varying the gear parameters listed in Tab. 1. For each gear, 10 samples were selected from random magnetic field rotations within the limits specified in Tab. 1. This results in 2,500 unique combinations of gear geometry and magnetic field configuration. The parameters for gear geometry and the magnetization direction of the support magnet were determined using the Latin Hypercube Sampling (LHS) strategy, which ensures a uniform distribution of sample points across the parameter space by dividing the parameter range into small segments and taking random samples from each segment [Loh96]. This approach ensures that no areas of the parameter space are over- or underrepresented, thereby improving data quality.

The training dataset comprises 2,500 unique samples. To ensure comprehensive parameter space coverage and reliable evaluation, an additional 250 gear-magnet combinations were simulated the specified parameter range. These simulations were used exclusively for testing, preserving the integrity of the training dataset during model development.

Tab. 1: Parameters describing the gear geometrics, magnetization and sensor position.

Variables	Range	Description
n	$\mathbf{26}$ ... $\mathbf{128}$	Number of teeth.
d	$\mathbf{16,55}\boldsymbol{mm}$ ... $\mathbf{81,49}\boldsymbol{mm}$	Pitch circle diameter of the gear.
s_p	$\mathbf{0,4}\boldsymbol{mm}$ ... $\mathbf{1,33}\boldsymbol{mm}$	Width of a tooth.
h	$\mathbf{0,5}\ \boldsymbol{mm}$ ... $\mathbf{2,0}\ \boldsymbol{mm}$	Height of a tooth.
$\Delta\Theta_x$	$\pm\mathbf{5}°$	Angle of rotation of the magnetic field around the $\boldsymbol{x}$-axis.
$\Delta\Theta_y$	$\pm\mathbf{5}°$	Angle of rotation of the magnetic field around the $\boldsymbol{y}$-axis.
t	$\mathbf{0,4}\ \boldsymbol{mm}$	Distance between GMR sensor and tooth surface.
Δx	$\pm\mathbf{200}\mu\boldsymbol{m}$	Offset of the GMR sensor along the $\boldsymbol{x}$-axis.
Δy	$\pm\mathbf{100}\mu\boldsymbol{m}$	Offset of the GMR sensor along the $\boldsymbol{y}$-axis.
$\Delta\varphi_z$	$\pm\mathbf{1}°$	Rotation of the GMR sensor around the $\boldsymbol{z}$-axis.

The training dataset is divided into training and validation data, with 80 % used as training data and 20 % as validation data. The validation dataset is used during model training to monitor performance and adjust the model's parameters, such as the weights, in order to optimize the learning process. To increase the training quality and numerical stability, the data is scaled to the 0 to 1 range using a min-max-scaler.

3.3 Signal and Parameter Analysis

The selection of suitable characteristics is an important step in the development of the model. Systematically varying specific tolerance parameters and analysing the sensor signals enables a deeper understanding of the system and creates the knowledge base for defining the model architecture and selecting relevant features.

Signal Analysis

To analyse the sensor signals, which resemble near-perfect sinusoidal signals, Fourier Transformation (FT) is employed to decompose the signals into their frequency components. This decomposition enables the identification of key features that are essential for understanding the sensor's behaviour under varying manufacturing tolerances. Specifically, the analysis focuses on the following features:

- Dominant amplitude: The magnitude of the largest amplitude, corresponding to the primary oscillation in the signal, is extracted to ignore potential noise and assess whether the amplitude exceeds predefined threshold values critical for sensor design and modeling. Higher-order harmonics are not considered, as their contribution is minor, and including them would unnecessarily increase the model's complexity.
- Average value: The mean signal level, which provides information on baseline shifts that may arise due to manufacturing deviations.

These features are selected to capture the most significant aspects of the signal's behaviour, facilitating a reduction in model complexity while preserving the essential information. By analysing these attributes, insights are gained into how specific manufacturing deviations influence the sensor's performance, thereby guiding the selection of relevant input variables for the subsequent ML model.

Parameter Analysis

The influence of the system parameters is analyzed before building the ML model. A correlation analysis is performed to locate and remove redundant parameters. This allows the complexity of the model to be reduced without adversely affecting the performance of the model.
Fig. 4 shows the correlation matrix with a reduced set of parameters from the dataset created for analysis. The values indicate the linear dependence between the parameters, with +-1 indicating positive/negative linear co-dependence, while 0 indicates no dependence at all. The results show a strong dependence between the diameter d and the number of teeth n. As the parameters are coupled via the fixed pitch of 2mm, the result was to be expected. Furthermore, a strong negative correlation of was observed between the signal averages a_0 of the sine and cosine signals. This indicates a mirrored behavior of the sensor signal averages, which reflects the symmetrical structure of the sensor.
In addition, a strong correlation between a_0 and the parameters n and d was observed. This correlation arises because smaller radii cause a stronger deflection of the magnetic field lines due to the gear solid, which increases the signal average.
The amplitudes $A_{1,sin}$ and $A_{1,cos}$ are correlated to the tooth width s_p. Basically, they result from the transition of the teeth beneath the sensor. Since reducing the tooth width s_p while keeping the pitch constant increases the size of the gap, the amplitudes of the sensor signal are affected. The 100% correlation between the amplitudes is due to the aforementioned mirror symmetry of the magnetic field lines and GMR sensor.

It is important to note that changes to the measurement system require a new correlation analysis, as correlation does not prove causality.

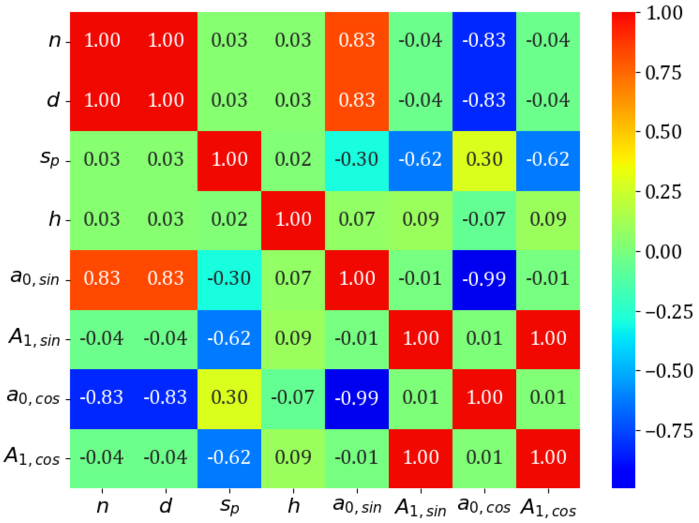

Fig. 4: Correlation matrix of a reduced set of parameters to find redundant information in the data.

3.4. Machine Learning Model Selection

Since the model is intended to predict the deviation in maximum amplitude and signal average between ideal and tolerance-affected sensor signals, as shown in Fig. 5, a regression model is required to be robust to the limited amount of simulation data. Simultaneously, the model should be capable of handling complex and nonlinear relationships between input and output values. Therefore, this study employs an Extreme Gradient Boosting (XGBoost) model [ChGu16].

XGBoost is a decision-tree-based model that iteratively adds new trees in a round-based manner to minimize the model's error. Its well-documented advantages make it particularly suited for this application. Important characteristics of XGB are [ChGu16]:

- Efficient handling of structured data and numerical features.
- Resistance to overfitting through regularization techniques.

- Fast training and prediction times.
- Capability to capture intricate interactions between input variables.

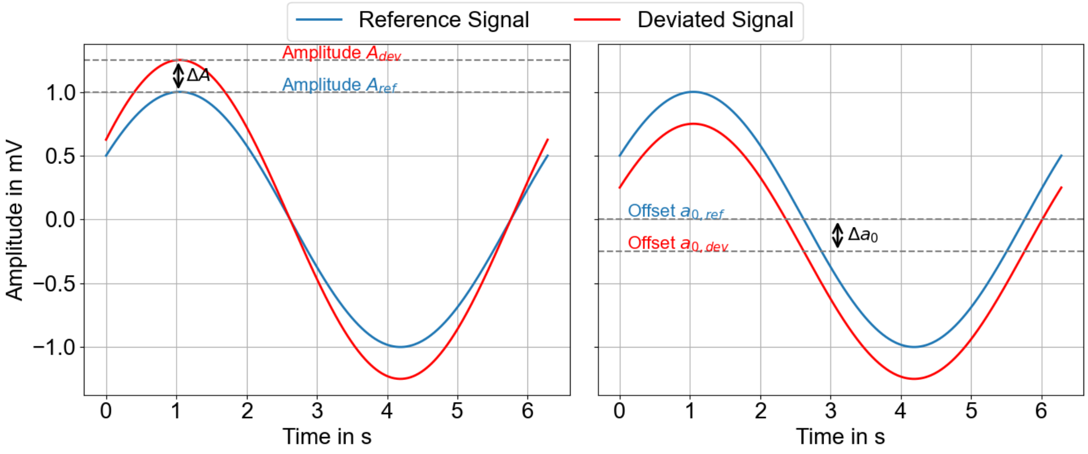

Fig. 5: The impact of variations in production-related parameters on sensor signals. The numerical parameters ΔA and Δa_0 are the model's target variables.

3.5 Hyperparameter Optimization

To improve the prediction performance of the XGBoost model, the hyperparameters are tuned using the Randomized Search method from the *sklearn.model_selection* library [BeBe12]. This approach enables the specification of bounds for each hyperparameter based on prior knowledge. Specifically, the hyperparameters are varied as shown in Tab 2.

Tab 2: Overview of the model's hyperparameters and their descriptions.

Hyperparameter	Description
Number of Estimators	The number of trees used in the model.
Learning Rate	Controls the weighting of the added trees after each training round.
Maximum Tree Depth	The maximum depth of each decision tree.
Subsample Ratio	The fraction of the training data used for growing each tree.
L1 Regularization	The L1 penalty applied to the weights to increase robustness.
L2 Regularization	The L2 penalty applied to all weights ensures numerical stability.

Within the defined bounds, randomly generated combinations of these hyperparameters are applied over a limited number of training iterations, following predefined step sizes. The performance of these combinations is evaluated by calculating prediction accuracy using standard error metrics such as mean squared error. This process allows the design of a pre-optimized model architecture tailored to the dataset, which is then employed for comprehensive training. Subsequently, the optimized model is evaluated on an unseen test dataset to assess its generalization capacity and prediction accuracy in estimating sensor signal deviations caused by manufacturing tolerances.

To reduce the risk of overfitting and to avoid unnecessary additional trees, the early stopping method is used. With this method, the training process can be stopped if no further improvements in the form of error reduction can be detected after a predefined number of iterations.

4. Results and Discussion

This chapter presents a comprehensive analysis of the effects of production-related deviations on the sensor signal, followed by the optimization of the model architecture using a hyperparameter random search algorithm. Subsequently, the model training is evaluated, and its performance on unseen data is tested. Finally, the findings of the study are summarized, and the applicability of the model in practical scenarios is proposed.

4.1 Impact of Manufacturing Tolerances on the Signal Response

In order to achieve a better understanding of the system, it is necessary to analyze the effect of production-related deviations in the sensor/magnet system on the sensor signal. In this section, simulation data representing systematic deviations within the specified tolerance limits is analyzed.

Sensor Offset in the x-Direction

When the sensor is shifted in the x-direction, two effects are expected to occur. Firstly, a phase shift is to be expected, but at this stage of the sensor design the only concern is to ensure that the maximum signal peaks, defined by level and amplitude, remain within the desired range. Secondly, the curvature of the gearwheel is expected to have an effect. The greater the curvature, the greater the effective distance between the sensor array and the tooth structure when the sensor array is displaced. An analysis of this phenomenon revealed that displacements in the horizontal direction have a greater effect on the signal average and amplitude for the smallest gear in the dataset than for the largest gear, by a factor of about 10. Since the model is designed to distinguish between the optimal sensor position and the sensor position constrained by tolerances, it is essential to evaluate different positions first.
The signal is expected to have the greatest amplitude when the sensor is centered. However, this expectation is not confirmed by the data, as shown in Fig. 6. Instead, the maximum values for signal average and amplitude are slightly off center. This phenomenon can be attributed to the configuration of the GMR elements as illustrated in Fig. 1. The center points of the GMR elements for the sine and cosine signal do not correspond to the center point of the sensor array.

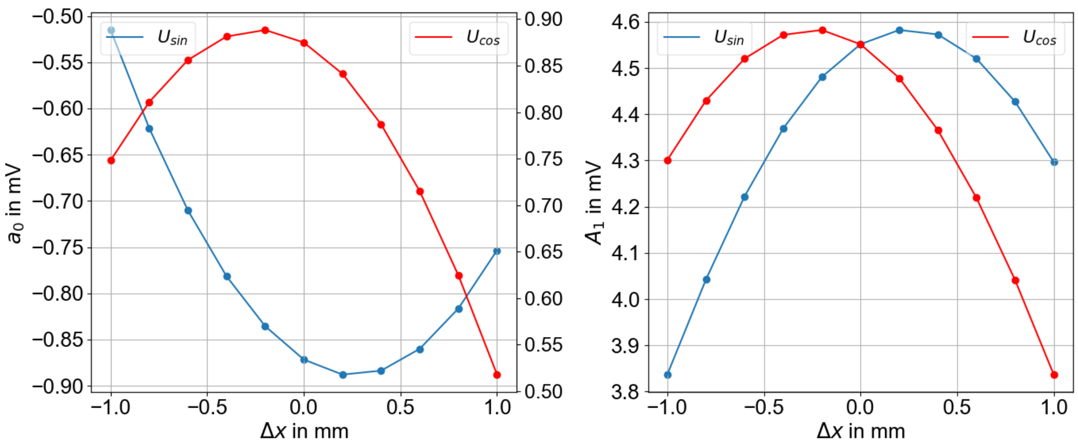

Fig. 6: The effect of sensor displacement Δx on signal amplitude and average.

Sensor Offset in the y-Direction

Moving the sensor array in the positive y-direction is expected to have the same effect as a gain in the working distance between the sensor magnet system and the tooth structure. The only difference is the constant position of the supporting magnet. Therefore, moving the sensor in the y-direction will result in an increase or decrease in the distance between the tooth structure and the GMR elements. This results in a significant change in the amplitude and average as shown in Fig. 7. It is noticeable that the curves for the average and amplitude have a nearly linear character in the considered range.

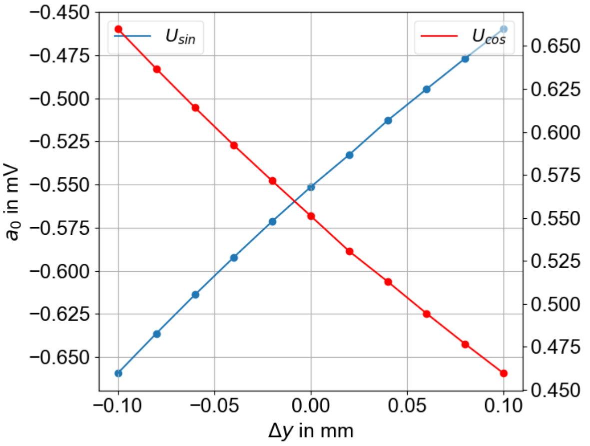

Fig. 7: The effect of sensor displacement Δy on signal amplitude and average.

Angles of Magnetization

In order to understand the influence of different magnetization angles on the sensor signal, a deep understanding of the interaction between GMR and magnetic field is necessary. However, this is not the subject of this work, as it is mainly concerned with modeling. In this context, it is important to know that the GMR sensor is sensitive to magnetic fields in the direction of the sensor-plane (horizontal plane). Since a rotation of the magnetic field changes the resulting magnetic field strength in horizontal direction, a change in the signals is recognizable. The range for the magnetization direction is specified as ±5° in each spatial direction of the coordinate system. Since the support magnet in this case is magnetized in the z-direction under perfect conditions, all rotation angles around the z-axis can be described by a combination of rotations around the x-axis and around the y-axis. For this reason, rotation angles around the z-axis are not considered. Fig. 8 shows the effects of deviating magnetization. It is noticeable that the behavior differs for rotation angles around the x-axis and around the y-axis. While rotations around the x-axis have a linear effect on amplitude and signal average, rotations around the y-axis have a non-linear character. Furthermore, the intensity with which the respective rotation influences the sensor signal differs. For example, a rotation around the x-axis has a factor of 10 greater effect than a rotation around the y-axis. The difference is even greater for the amplitude, where rotations around the x-axis have a factor of 26 greater influence.

Sensor Rotation around the z-axis

As demonstrated in Fig. 9, the rotation of the sensor array influences the sensor signal, leading to a linear change in signal amplitude with varying rotation angles. However, the signal average follows a cubic trend with inflection points at 0° rotation, corresponding to the sensor being exactly horizontal in space. This behavior can be attributed to the specific configuration of the GMR elements along the sensor axis, where each pair of elements is aligned vertically. As the inner GMR elements 3 and 4 are positioned on the opposite side of the sensor's center relative to the outer elements 7 and 8, rotation increases the distance of the outer elements from the tooth surface while simultaneously decreasing the distance of the inner elements. This results in a rotation of the effective horizontal field components acting on each element and height differences between inner and outer GMR elements. Since the magnetic field strength decreases with increasing distance from the tooth surface, these height variations further contribute to the observed signal changes.

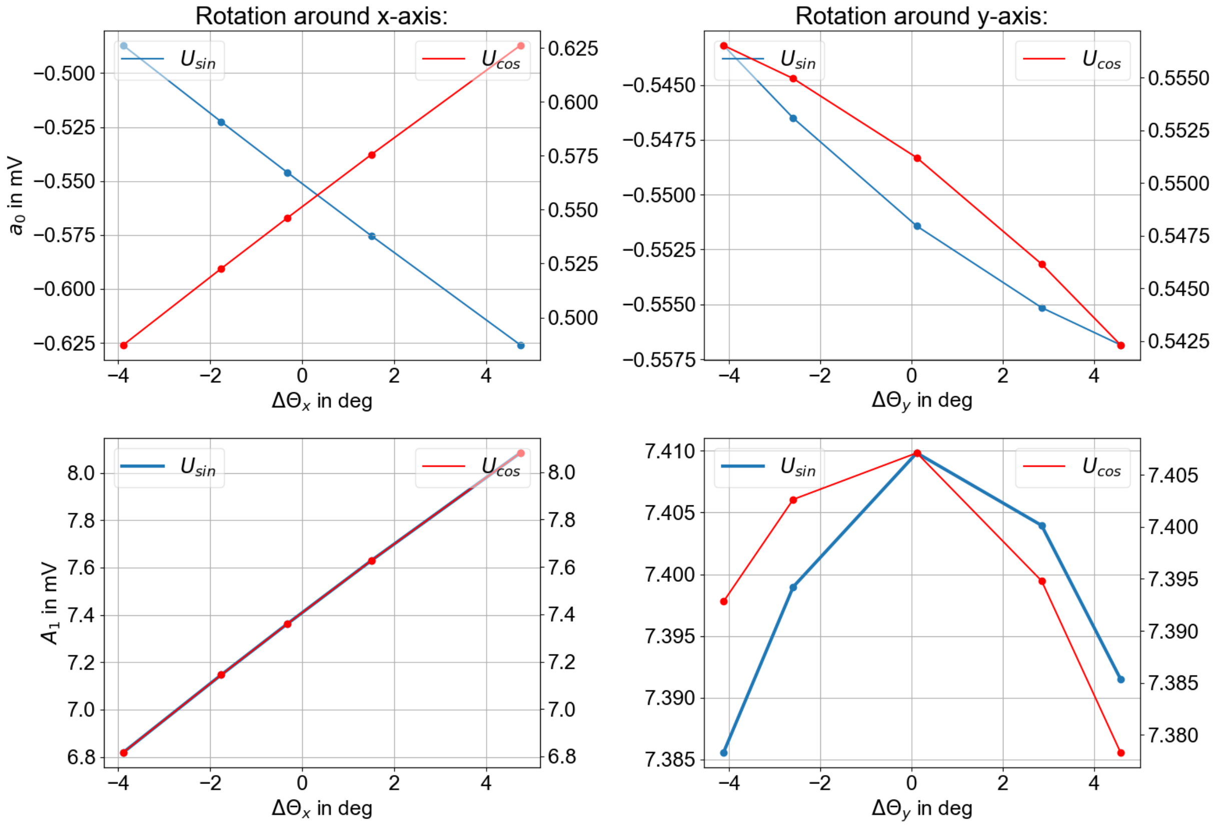

Fig. 8: The influence of magnetization angle deviations Θ_x and Θ_y on signal amplitude and average.

The increase in the sine signal amplitude and the simultaneous decrease in the cosine signal amplitude can therefore be attributed to both the lateral displacement of the GMR elements within the sensor array and the height-dependent modulation of the effective field.

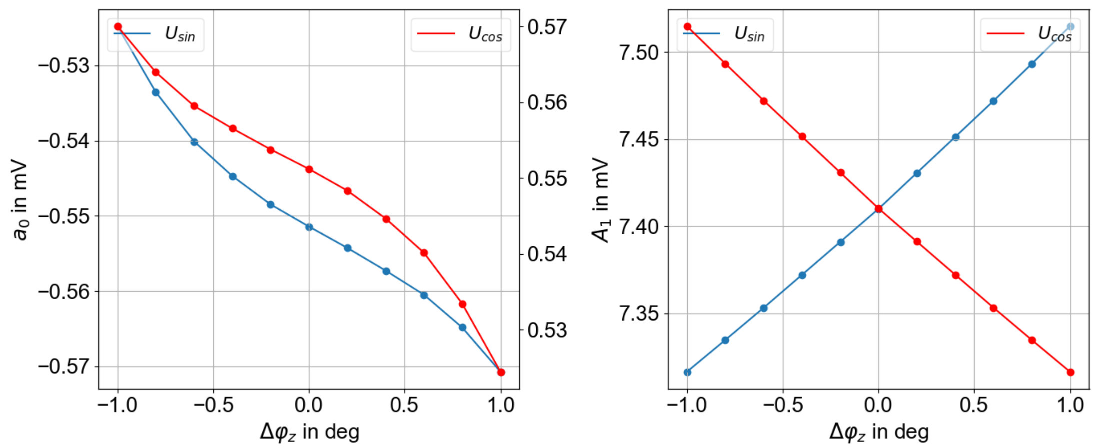

Fig. 9: The effect of sensor rotation $\Delta\varphi_z$ on signal amplitude and average.

4.2 Model Performance and Architecture

This section evaluates the performance of the model. First, the parameters obtained from the hyperparameter search are presented. This gives an overview of the architecture of the model and shows the extent of regularization used. The training results are presented afterwards, followed by an evaluation on unknown data, which allows the generalizability of the model to be assessed. Finally, the results of this work are categorized and possible applications of the model are discussed.

Hyperparameters and Architecture

Tab. 3 presents the results of the hyperparameter search. The model initially consists of fifty thousand trees with a depth of 3. Since the model training employs an early stopping method, this number may be reduced in the final model. Another important observation from the table is the learning rate, which is set to 0.01. However, it also implies a higher need for additional trees to converge, which could lead to overfitting. This indicates the importance of stopping early.

Tab. 3: Optimized Hyperparameters from Randomized Search Method.

Hyperparameter	**Value**	**Search Range**
Number of Estimators	50000	100 … 75000
Learning Rate	0,013	0,01 … 1,00
Maximum Tree Depth	3	1 … 10
Subsample Ratio	0,8	0,1 … 1
L1 Regularization	0,1	0 … 1
L2 Regularization	6	0 … 10

Furthermore, the hyperparameter search identified a subsample ratio of 0.8, indicating that 80% of the training data is used for building each tree. This helps balancing between model robustness and computational efficiency. Regarding regularization, the L1 regularization parameter is set to 0.1, which promotes a certain degree of sparsity in the model structure. In contrast, the L2 regularization parameter is set to 6, enforcing stronger penalties on large coefficient values to improve model stability and reduce overfitting risks [ChGu16].

Model Performance

Before evaluating the model, the analyzing of the training results provides valuable insights. In addition to the familiar metrics such as the mean squared error, this also includes recognizing whether or not the number of additional trees has been reduced by using early stopping. A significant deviation in the number of trees may indicate a problem with the optimized hyperparameters found by the search algorithm. Experience has shown that an excessive deviation between the optimum number of trees and the number of trees from the hyperparameter search indicates that the hyperparameter search has not found the optimum configuration. In such a case, the limits and the number of iterations in the hyperparameter search are adjusted and this is carried out again. In the case of this model, the search determined an initial tree number of 50000 and the early-stopping algorithm cancelled the training after 46625 rounds. The difference between the two values indicates no need for change.

Another important information is the relevance of the parameters during model training, which can be seen in Fig. 10. The parameter $\Delta \boldsymbol{y}$ was almost twice as useful for model prediction as the next most important parameter. The parameter $\boldsymbol{\Theta_y}$, which represents the rotation of the magnetic field around the $\boldsymbol{y}$-axis, has the least benefit for the model. This information is consistent with the analysis from Section 4.1.

To evaluate the model training, the mean squared error was documented after each training lap. By looking at this metric, it is possible to assess whether the model is converging during training, or whether the model is struggling to recognize the relationships and patterns in the dataset. The model from this work achieved a R2 score of 0.9978 on the training data, which indicates a high model quality. However, in order to make more precise statements about the model performance, it is necessary to apply the model to unknown data.

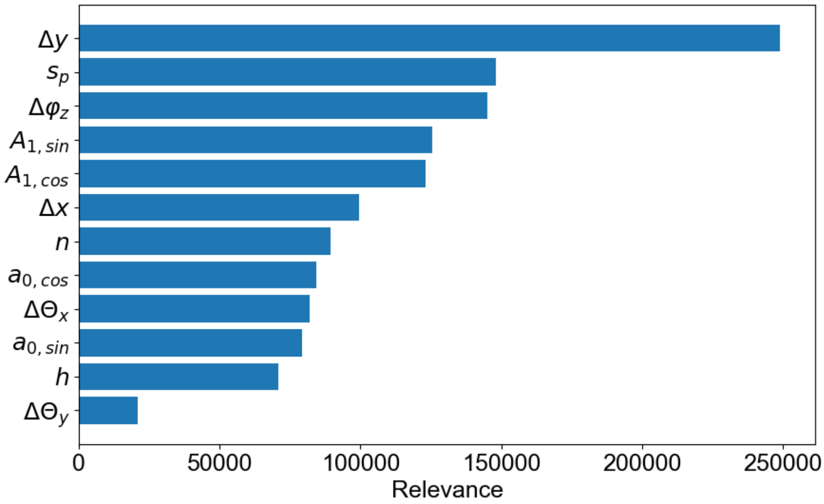

Fig. 10: Parameter relevance shows how important a particular parameter was to the model during training.

Model Performance when Using Unknown Data

The test dataset used for this project was created from new randomly generated simulations within the specified limits for the production-related deviations. The evaluation metric used was the percentage deviation from the actual values and the predicted values. The model was therefore able to achieve the deviation between the ideal sensor signal and the tolerance-based sensor signal with an average accuracy of 99.61 %. In order to view the model performance from a different angle, a parity plot is shown in Fig. 11.

The model was able to determine the deviation of the amplitude more accurately than the deviation of the signal average.

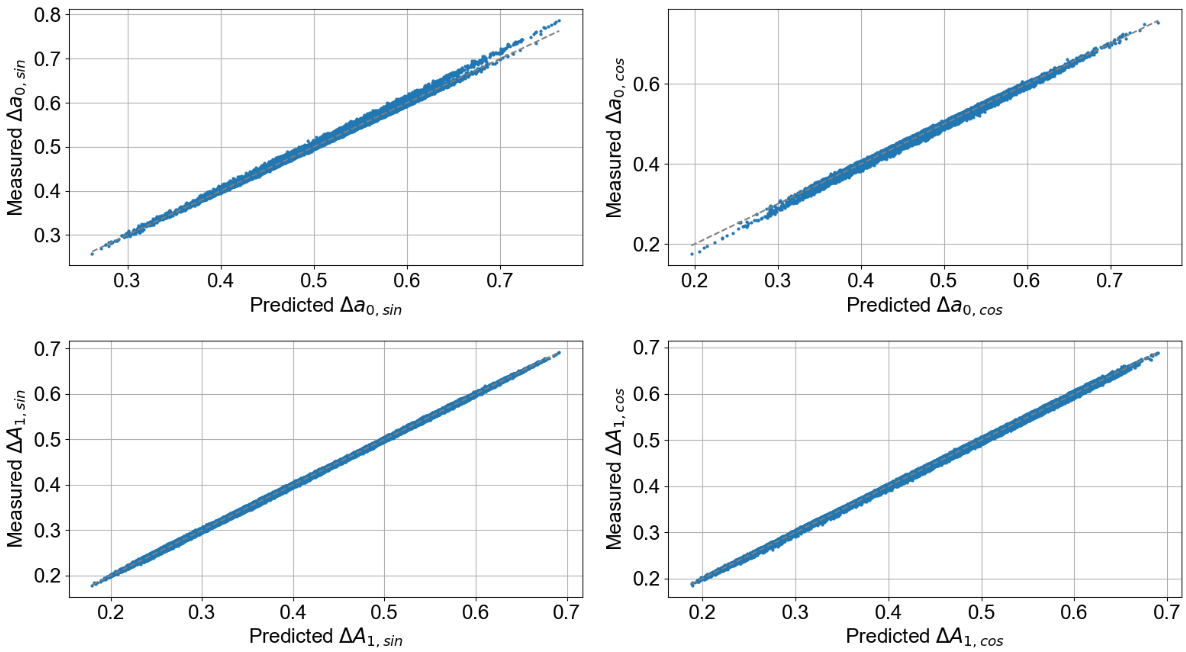

Fig. 11: Parity Plot of the model.

4.3 Outlook and Applications

The objective of this study was to develop an ML-based model to predict the effects of production-related deviations on the performance of simulated sensor signals. To achieve this, simulated training data was generated using FEM simulations. The study included a detailed analysis of the influence of manufacturing tolerances on the sensor signal, an evaluation of the correlations between parameters using a correlation matrix, and the development and implementation of an XGBoost model. Model validation on previously unseen data showed that the target parameters (signal average deviation and signal amplitude deviation) can be predicted with an average accuracy of 99.61%. The results also indicate that the model has a higher prediction accuracy for signal amplitude deviation than for signal average deviation in the considered use case.

These results demonstrate the potential of using ML models to approximate computationally intensive FEM simulations and to quantify the influence of manufacturing tolerances on sensor performance. The approach developed enables sensor designers to estimate the effect of manufacturing variations during the design phase and to reduce the need for time-consuming FEM simulations. This allows for more efficient optimization of sensor placement and parameters. However, further investigations are required to test the extrapolation capability of the model.

Acknowledgement

This work has been developed within the project “Basissystem für unternehmensübergreifende Produktionsunterstützung”. ”BaSys ¨uberProd”(reference number: 01—S20094T) is funded by the German ministry of education and research (BMBF) as part of the BaSys 4.2 research program. It is an application project that uses the technologies developed in the BaSys 4.0 and BaSys 4.2 projects to realise reusable solutions for Industry 4.0 in concrete application contexts. These solutions will be made available as reusable containers in order to make them usable for a broad mass of users. In this way, smaller companies, for example, can also benefit from AI solutions and use them with little effort. The responsibility for the content of this publication lies with the author.

SPONSORED BY THE
Federal Ministry of Education and Research

Literature

[AhUd23] AHAMED, SABBER ; UDDIN, MD MESBAH: Addressing computational challenges in physical system simulations with machine learning, arXiv (2023). — arXiv:2305.09627 [physics]

[BeBe12] BERGSTRA, JAMES ; BENGIO, YOSHUA: Random search for hyper-parameter optimization. In: *J. Mach. Learn. Res.* Bd. 13, JMLR.org (2012), Nr. null, S. 281–305

[ChGu16] CHEN, TIANQI ; GUESTRIN, CARLOS: XGBoost: A Scalable Tree Boosting System. In: *Proceedings of the 22nd ACM SIGKDD International Conference on Knowledge Discovery and Data Mining*. San Francisco California USA : ACM, 2016 — ISBN 978-1-4503-4232-2, S. 785–794

[GLHX21] GAO, YUN ; LIU, XIAOYANG ; HUANG, HAIZHOU ; XIANG, JIAWEI: A hybrid of FEM simulations and generative adversarial networks to classify faults in rotor-bearing systems. In: *ISA Transactions* Bd. 108 (2021), S. 356–366

[LiHX20] LIU, XIAOYANG ; HUANG, HAIZHOU ; XIANG, JIAWEI: A Personalized Diagnosis Method to Detect Faults in a Bearing Based on Acceleration Sensors and an FEM Simulation Driving Support Vector Machine. In: *Sensors* Bd. 20 (2020), Nr. 2, S. 420

[Loh96] LOH, WEI-LIEM: On Latin hypercube sampling. In: *The Annals of Statistics* Bd. 24 (1996), Nr. 5

[ReCR09] Reig, Càndid ; Cubells-Beltrán, María-Dolores ; Ramírez Muñoz, Diego: Magnetic Field Sensors Based on Giant Magnetoresistance (GMR) Technology: Applications in Electrical Current Sensing. In: *Sensors* Bd. 9 (2009), Nr. 10, S. 7919–7942

[Schö14] Schöberl, Joachim: C++ 11 implementation of finite elements in NGSolve. In: *Institute for analysis and scientific computing, Vienna University of Technology* Bd. 30, Citeseer (2014)

[Schö97] Schöberl, Joachim: NETGEN An advancing front 2D/3D-mesh generator based on abstract rules. In: *Computing and visualization in science* Bd. 1, Springer (1997), Nr. 1, S. 41–52

[WaYX22] Wang, Hui ; Yang, Ronggang ; Xiang, Jiawei: Numerical simulation of gears for fault detection using artificial intelligence models. In: *Measurement* Bd. 203 (2022), S. 111898